Developmental Biology **216,** 85–97 (1999)
Article ID dbio.1999.9497, available online at http://www.idealibrary.com on IDEAL®

Pattern Central Projections of Sensory Axons within the Cranial Mesenchyme of the Developing Mouse

Jon P. Golding,[1] Hester Tidcombe, Stavroula Tsoni, and Martin Gassmann

Division of Neurobiology, National Institute for Medical Research, The Ridgeway, Mill Hill, London NW7 1AA, United Kingdom

During mammalian hindbrain development, sensory axons grow along highly stereotyped routes within the cranial mesenchyme to reach their appropriate entry points into the neuroepithelium. Thus, trigeminal ganglion axons always project to rhombomere (r)2, whilst facial/acoustic ganglia axons always project to r4. Axons are never observed to enter the mesenchyme adjacent to r3, raising the possibility that r3 mesenchyme contains an axon growth-inhibitory activity. Conversely, in mice which lack the erbB4 receptor (normally expressed in r3), trigeminal and facial/acoustic ganglia axons misproject into r3 mesenchyme, suggesting that the putative axon barrier is absent. To investigate this hypothesis, we have developed an *in vitro* model in which dissociated wild-type embryonic trigeminal ganglion neurons are cultured on longitudinal cryosections of embryonic mouse head. We observed that on wild-type embryonic day 10 (E10) cryosections, neurites generally failed to grow into r3 mesenchyme from the adjacent r2 or r4 mesenchyme. This barrier was removed if cryosections were pretreated with chondroitinase or were washed with excess chondroitin 6-sulphate or hypertonic saline. By contrast, when trigeminal neurons were seeded onto cryosections of E10 erbB4 −/− embryo heads their neurites readily entered mutant r3 mesenchyme. Immunohistochemical analysis demonstrated chondroitin-sulphated proteoglycans throughout the cranial mesenchyme in both wild-type and erbB4 −/− embryos. We propose that trigeminal axons are excluded from wild-type r3 mesenchyme by a growth-inhibitory activity which associates with chondroitin-sulphated proteoglycans and that the synthesis of this activity may rely on signals transduced by erbB receptors.

Key Words: **hindbrain; trigeminal ganglion; axon growth inhibition; proteoglycans; erbB4.**

INTRODUCTION

During development, growing axons are constrained to appropriate pathways by combinations of growth-promoting and growth-inhibitory cues within the surrounding tissues and also by neuronal changes in the responsiveness of growth cones to these various guidance cues (Keynes *et al.*, 1997; Walsh and Doherty, 1997; Chiba and Keshishian, 1996; Culotti and Kolodkin, 1996; Nieto, 1996; Keynes and Cook, 1995). In the developing vertebrate hindbrain, it remains unclear which of these mechanisms predominate in dictating how centrally projecting sensory axons from individual ganglia navigate to their well-defined entry sites into the neuroepithelium. It has been suggested that the transient segmentation of the hindbrain neuroepithelium along its anteroposterior axis into metameric compartments called rhombomeres (r) regulates the segmented pattern of cranial sensory ganglia and their nerves (Lumsden and Krumlauf, 1996). Because cranial ganglia form immediately adjacent to the rhombomere they will innervate, one possibility is that short-range chemoattractive cues are released by neural crest-derived boundary cap cells which populate the presumptive axon entry sites in r2, r4, and r6 (Niederlander and Lumsden, 1996). However, cocultures of hindbrain and cranial ganglia have so far failed to detect any chemoattractive activity for sensory axons (Tucker *et al.*, 1996). Another possibility is that repulsive cues exist within the mesenchyme or neuroepithelial basal lamina between neighbouring entry sites to constrain axons to enter their appropriate rhombomere (Keynes *et al.*, 1991).

[1] To whom correspondence should be addressed. Fax: +44-181-913-8523. E-mail: jgoldin@nimr.mrc.ac.uk.

0012-1606/99 $30.00

One such candidate repulsive activity are chondroitin-sulphated proteoglycans (CSPGs), which have been found at high concentrations in several areas of developing vertebrates that act as barriers to axon growth and cell migration (Silver, 1994; Oakley and Tosney, 1991; Snow *et al.*, 1991). Some CSPGs are known to directly inhibit growth (Fernaud-Espinosa *et al.*, 1998), whilst others act indirectly by binding to, and thereby modulating the effects of, various cell adhesion molecules and growth factors (Grumet *et al.*, 1996; Margolis and Margolis, 1997). However, the presence of CSPGs does not always correlate with the restriction of axon growth, since some CSPGs are reported to stimulate neurite growth (Faissner *et al.*, 1994). Another class of sulphated proteoglycans, heparan sulphate proteoglycans (HSPGs), are found in association with basement membranes in the developing vertebrate nervous system (Walz *et al.*, 1997; Treloar *et al.*, 1996) and various members either have a slight inhibitory effect (Tonge *et al.*, 1997) or a stimulatory effect (Hantaz-Ambroise *et al.*, 1987) on axon growth, most likely by sequestering or presenting various growth factors (Walz *et al.*, 1997).

Further insight into the mechanisms which pattern cranial axon projections can be gained from studies of mutant mice, lacking certain segmentally expressed transcription factors. Thus, in mice lacking Hoxa-2 (Gavalas *et al.*, 1997), Hoxb-1 (Studer *et al.*, 1996), or Krox20 (Schneider-Maunoury *et al.*, 1997), misrouting of cranial motor axons is observed, apparently as a result of rhombomere deletions and/or respecification of rhombomere identity. Another mutant mouse, which lacks the erbB4 receptor tyrosine kinase (a receptor for neuregulin), shows axon pathfinding defects in the hindbrain, although rhombomeric segmentation and identity appear to be unaffected (Gassmann *et al.*, 1995). Furthermore, in erbB4 −/− mutants it was observed that mistargeting of axons is not only confined to motor neurons, but also affects the central projections of trigeminal and facial/acoustic sensory ganglia. Thus, trigeminal ganglion axons grow to their appropriate entry site in r2, but also grow inappropriately through r3 mesenchyme to the entry site in r4. Similarly, facial/acoustic ganglia axons grow to their appropriate entry site in r4 but also grow via r3 mesenchyme to the trigeminal entry site in r2 (Gassmann *et al.*, 1995). This observation raises the possibility that wild-type r3 mesenchyme contains an axon growth-inhibitory activity whose synthesis is regulated by erbB4 signalling within r3 and is therefore absent in erbB4 −/− embryos. In this study we use a cryoculture technique to demonstrate that wild-type (but not erbB4 −/−) r3 mesenchyme indeed contains a barrier to axon growth at an appropriate time during hindbrain development to influence the central projections of trigeminal and facial/acoustic sensory neurons. Furthermore, we provide evidence that the r3 mesenchyme neurite growth inhibitor might be presented to the axons by chondroitin-sulphated proteoglycans within the cranial mesenchyme.

MATERIALS AND METHODS

Animals

A *neo* cassette was inserted into exon 2 of the mouse *erbB4* gene by homologous recombination, thereby rendering the gene product nonfunctional (Gassmann *et al.*, 1995). A breeding colony of heterozygous erbB4 +/− mice was maintained at NIMR and the erbB4 −/− genotype of embryos was confirmed by PCR analysis of yolk-sac DNA using erbB4-specific primers (Gassmann *et al.*, 1995). Wild-type CBA mice were obtained from a breeding colony at NIMR.

Cryoculture

Wild-type E8–E10 or erbB4 −/− E10 embryos were bisected along a line parallel with the dorsal surface of the hindbrain, from the thorax to the forebrain (Fig. 1A). The dorsal half of each embryo was mounted on card, dorsal surface uppermost, in a thin smear of cryoembedding compound (Bright) and was snap frozen in liquid nitrogen. Longitudinal 10-μm cryosections were collected on sterile polylysine-coated glass coverslips (13 mm diameter; Chance Propper) and stored at −70°C for up to 2 weeks (Fig. 1A).

Trigeminal ganglia or the ventral third of r2 plus r3 neuroepithelium (containing trigeminal motor neurons and interneurons) or telencephala were dissected from E10 wild-type embryos in DMEM, digested with 500 μl 11 U/ml trypsin (Worthington) for 10 min at 37°C, washed in three changes of DMEM, and triturated in 30 μl of 0.25 mg/ml soybean trypsin inhibitor type II (Sigma) plus 0.05 mg/ml DNase type I (Sigma) in Hanks' balanced salts (Gibco). Dissociated cells were diluted to 20,000 cells/ml in F14 medium (Davies, 1996) containing 10 ng/ml NT-3 and 10 ng/ml BDNF (R&D Systems). Coverslips bearing head cryosections were placed individually into four-well culture dishes (Nunc) and 500 μl of cell suspension was added to each well (Fig. 1A). Cultures were maintained in a humidified atmosphere of 5% CO_2 and 95% air at 37°C for 18 h and then fixed with 2% paraformaldehyde for 15 min and permeabilized with methanol for 3 min. Cryocultures were dual immunostained with rabbit anti-laminin (1:200; Sigma), to allow identification of the rhombomeres, and mouse monoclonal anti-β3-tubulin (TUJ1, 1:1000; BAbCO, Richmond), to identify applied neurons and their neurites. Primary antibodies were visualised with Cy2-conjugated anti-rabbit Ig and Cy3-conjugated anti-mouse Ig secondary antibodies (both 1:200; Amersham) and counterstained with DAPI nuclear stain (5 μg/ml, Sigma). Cryocultures were mounted on glass slides in Glycergel (DAKO) and photographed using an epifluorescence microscope (Zeiss).

Modifications of Cryoculture Conditions

In some experiments, cryosections were pretreated with various solutions and then extensively washed with PBS before applying dissociated trigeminal ganglion neurons and culturing overnight. These pretreatments included 100 μl chondroitin sulphate-A (CS-A, 25 mg/ml in PBS, Sigma) for 2 h at 37°C; 100 μl chondroitin sulphate-C (CS-C, 25 mg/ml in PBS, Sigma) for 2 h at 37°C; 100 μl heparin (grade 1-A sodium salt, 25 mg/ml in PBS, Sigma) for 2 h at 37°C; 100 μl 0.5 M NaCl (in phosphate buffer, pH 7.2) for 2 h at 37°C; 30 μl chondroitinase ABC (CH-ase, EC 4.2.2.4, 6 U/ml in 50 mM Tris–HCl, pH 8.0, containing 400 μg/ml BSA, Oxford GlycoSciences) for 5 h at 37°C; 30 μl of CH-ase buffer only for 5 h at 37°C as a control; 30 μl hyaluronidase (EC 3.2.1.35, 5 U/ml in 0.1 M

sodium acetate buffer, pH 5, ICN) for 4 h at 37°C; 30 μl heparitinase (EC 4.2.2.8, 0.5 U/ml in 2.5 mM calcium acetate, pH 7, ICN) for 4 h at 37°C; 60 μl phosphatidylinositol phospholipase C (Pi-PLC, EC 3.1.4.10, 10 U/ml in PBS, Oxford GlycoSciences) for 3 h at 37°C; or 100 μl PBS for 2 h at 37°C as a control. In some experiments the culture medium was supplemented with a mouse monoclonal antibody to the extracellular domain of erbB4 (clone H4.72.8, 1:40, 5 μg/ml, Neomarkers), previously shown to block the binding of neuregulin to erbB4 (Chen *et al.*, 1996), or a 1:40 dilution of normal mouse serum as a control. After culturing with dissociated neurons, all cultures were fixed and dual immunostained with anti-laminin and anti-β3-tubulin antibodies, as described.

Statistical Analysis of Neurite Interactions with Cryosections

In immunostained cryocultures, mesenchyme adjacent to the rhombomeres was divided into segments by extending an imaginary line out from each rhombomere boundary, perpendicular to the neuraxis. Neurites which encountered the boundaries between r2, r3, or r4 mesenchymal segments were quantified as follows: The number of neurites which extended by more than 20 μm onto r3 mesenchyme from r2 or r4 mesenchyme was expressed as a percentage of the total number of neurites within r2 or r4 mesenchyme which encountered the r3 mesenchyme boundary. Conversely, the number of neurites which extended onto r2 or r4 mesenchyme from r3 mesenchyme was expressed at a percentage of the total number of neurites within r3 mesenchyme which encountered the boundary with r2 or r4 mesenchyme. Each experimental condition was repeated on three to nine independent occasions to produce a mean value for the percentage of neurites entering or leaving r3 mesenchyme. A two-tailed Student's *t* test was used to determine the significance of any differences between the mean percentages derived from each experimental condition. When multiple comparisons were made to a single control value, the *t* test was subject to sequential Bonferroni corrections.

Creation of Artificial Substrate Boundaries in Vitro

A mixture of Protein A (5 mg/ml, Sigma) and fluoresceinated latex beads (1:500, 50 nm diameter, Polysciences) in PBS was dispensed as discrete 5-μl spots onto polylysine-coated glass coverslips, incubated for 2 h at 25°C and then washed in 3 × 1-ml changes of PBS. Nonspecific binding was blocked by adding 500 μl of DMEM containing 10% FCS (DMEM/F10) for 1 h. This was then replaced for 2 h with 400 μl of DMEM/F10 containing 2 μg/ml of a fusion protein comprising the human immunoglobulin Fc domain and the extracellular domain of mouse erbB4 (a gift of Yosef Yarden, Weizmann Institute, Rehovot, Israel). Control coverslips were instead incubated with 2 μg/ml of human IgG (Sigma). All coverslips were washed with three changes of DMEM, seeded with 500 μl of trigeminal ganglia cell suspension, and cultured overnight. We confirmed that protein A-treated areas of coverslips bound erbB4-Fc and human IgG by immunostaining with an HRP-conjugated anti-human Ig $F(ab')_2$ fragment antibody (1:500, Amersham). The proportion of neurites which grew into the erbB4-Fc or control IgG-coated areas was counted on an epifluorescence microscope, equipped with phase contrast optics.

Immunohistochemistry

Some cryosections were fixed with 4% paraformaldehyde and then washed with PBS, blocked with 10% skimmed milk powder in PBS for 1 h, and immunostained with either a mouse monoclonal anti-chondroitin sulphate proteoglycan antibody (clone CS-56, 1:200; Sigma) or a rat monoclonal anti-heparan sulphate proteoglycan (perlecan core protein) antibody (clone A7L6, 1:300; Chemicon), followed by either Cy3-conjugated anti-mouse Ig secondary antibody (1:200; Amersham) or Cy-2-conjugated anti-rat Ig secondary antibody (1:200; Amersham), respectively, and 5 μg/ml DAPI nuclear stain (Sigma). Other cryosections were immunostained with a mouse monoclonal anti-chondroitin-6-sulphate proteoglycan (C6SPG) antibody (1:500; ICN), which specifically recognises the attachment site of C6S to the core protein and therefore requires this epitope to be unmasked by predigesting unfixed cryosections with 6 U/ml CH-ase for 4 h at 37°C. Treated cryosections were then washed and fixed with 4% paraformaldehyde before being blocked and incubated with anti-C6SPG. Control sections, which were not predigested with CH-ase, did not demonstrate any immunoreactivity with anti-C6SPG.

In Situ Hybridisation

A plasmid, containing a 600-bp amino-terminal-encoding erbB4 cDNA (Gassmann *et al.*, 1995), was used for the preparation of antisense digoxigenin-labelled riboprobe. Whole mount *in situ* hybridisation was performed on E9–E10 wild-type and erbB4 −/− embryos, using 400 ng/ml riboprobe, according to the method of Wilkinson and Nieto (1993). Transverse vibratome sections were cut through some embryos after staining.

RESULTS

Trigeminal Neurites Avoid Entering Wild-Type r3 Mesenchyme

Dissociated wild-type E10 trigeminal ganglion neurons were cultured overnight on longitudinal cryosections of wild-type E8–E10 head, which were subsequently immunostained with anti-laminin and anti-β3-tubulin antibodies. On all ages of hindbrain substrate, neurons attached randomly and extended bipolar neurites. Outside the neuroepithelium, neurites were seen to grow both within the mesenchyme and along the pial basal lamina (Figs. 1B–1D). Initially, we examined how neurites growing alongside the neuroepithelium on E10 cryosections behaved at the boundaries between r2 and r3 mesenchyme and between r3 and r4 mesenchyme. Neurites seldom grew onto r3 mesenchyme from r2 mesenchyme or r4 mesenchyme (32.4 ± 4.7%, 129 neurites, $n = 9$), although neurites readily grew in the opposite direction, from r3 mesenchyme onto r2/r4 mesenchyme (75.2 ± 5.3%, 114 neurites, $n = 9$; $P < 0.0001$) (Fig. 1D). Neurites which failed to grow onto r3 mesenchyme generally remained at the mesenchymal boundary, as if paralysed, although their growth cones were rarely collapsed. However, a small population of neurites were observed to have turned around and continued growing away from r3 mesenchyme (15 of 84 neurites examined).

To define the onset of the neurite growth-inhibitory

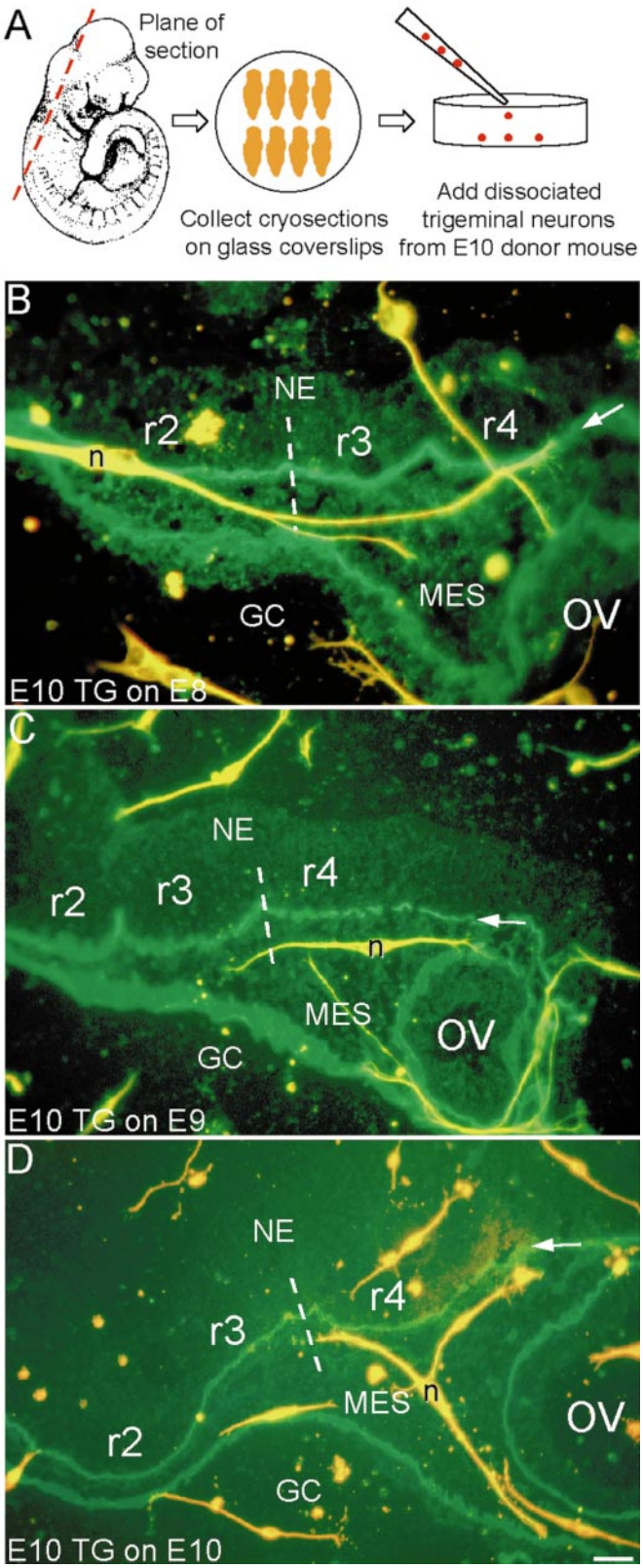

activity within r3 mesenchyme, we seeded E10 neurons onto E9 and E8 head cryosections and found that the barrier to neurite growth onto r3 mesenchyme became progressively weaker on younger cryosections. On E9 cryosections 54.2 ± 8.0% of neurites (75 neurites, $n = 4$) grew from r2 or r4 mesenchyme onto r3 mesenchyme (Fig.1C); whilst on E8 cryosections 71.4 ± 2.8% of neurites (37 neurites, $n = 3$) grew onto r3 mesenchyme (Fig. 1B). The proportion of neurites which grew in the opposite direction, from r3 mesenchyme onto r2/r4 mesenchyme, also increased as the age of the hindbrain substrate was decreased, being 76.3 ± 9.1% (70 neurites, $n = 4$) on E9 cryosections and 92.6 ± 7.4% (19 neurites, $n = 3$) on E8 cryosections. However, the mean length of neurite growth on the cryosections was not significantly influenced by the age of the substrate, being 57.3 ± 2.6 μm on E8 cryosections, 61.2 ± 3.9 μm on E9 cryosections, and 51.3 ± 4.2 μm on E10 cryosections (100 neurites measured in each case).

To determine whether neurites from other classes of neuron were similarly sensitive to the r3 mesenchyme growth-inhibitory activity, we seeded wild-type E10 head cryosections with dissociated E10 neurons, isolated either from the basal plate of r2/r3 hindbrain neuroepithelium (mostly motorneurons, whose peripheral processes would normally encounter r3 mesenchyme) or telencephalic neurons (whose axons would normally not encounter any mesenchyme adjacent to the hindbrain). Hindbrain neurons were found to be sensitive to the growth-inhibitory activity of r3 mesenchyme, with only 35.7 ± 10.7% of their neurites entering r3 mesenchyme from r2 or r4 mesenchyme (15 neurites, $n = 3$), whilst these neurites readily grew out of r3 mesenchyme onto the adjacent r2/r4 mesenchyme (82.2 ± 4.9%, 21 neurites, $n = 3$; $P < 0.02$) (Fig. 2A). By contrast, telencephalic neurons were unaffected by r3 mesenchyme, with 67.2 ± 16.8% of neurites growing into r3 mesenchyme from r2 or r4 mesenchyme (18 neurites, $n = 3$) and 56.5 ± 10.8% of neurites growing out of r3 mesenchyme onto the adjacent r2/r4 mesenchyme (19 neurites, $n = 3$) (Fig. 2B).

FIG. 1. Mesenchyme adjacent to r3 becomes nonpermissive to sensory axon growth between E8 and E10 in wild-type mouse embryos. (A) Longitudinal cryostat sections of E8–E10 embryo head were collected on polylysine-coated glass coverslips and used as a substrate for the growth of E10 dissociated trigeminal ganglion neurons. (B–D) Cultures were maintained overnight and then fixed and immunostained with anti-laminin antibody (shown in green) and anti-β3-tubulin antibody (orange), to reveal hindbrain structures and applied neurons (n), respectively. From E8 (B), E9 (C), to E10 (D) the proportion of E10 neurites which extended from r2 mesenchyme or r4 mesenchyme onto r3 mesenchyme (boundary marked by dashed line) declined progressively. NE, neuroepithelium; MES, mesenchyme; GC, glass coverslip; OV, otic vesicle. Arrows mark the line of the laminin-rich neuroepithelial basal lamina. Bar, 50 μm.

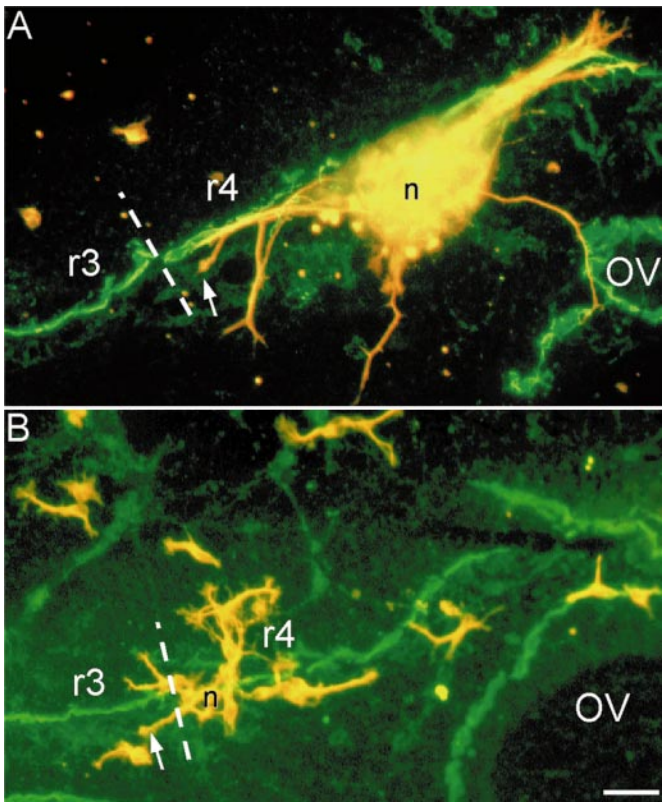

FIG. 2. Hindbrain motorneurons, but not telencephalic neurons are sensitive to the r3 mesenchyme growth inhibitor. E10 wild-type head cryosections (stained green by anti-laminin antibody) were seeded with dissociated neurons (n), derived from either E10 r2 plus r3 ventral neuroepithelium (A) or E10 telencephalon (B). Neurons and growing neurites are stained orange with anti-β3-tubulin antibody. In A hindbrain motorneurons avoid growing neurites into r3 mesenchyme from the adjacent r4 mesenchyme (arrow), whilst in B telencephalic neurons are able to grow neurites into r3 mesenchyme (arrow). The boundary between r3 and r4 mesenchyme is marked with a dashed line. OV, otic vesicle. Bar, 50 μm.

Some Pretreatments of Cryosections Disrupt the r3 Mesenchyme Growth-Inhibitory Activity

Pretreatment of wild-type E10 head cryosections with either CH-ase, CS-C (composed chiefly of chondroitin 6-sulphate chains), or hypertonic saline all significantly reduced the axon growth inhibitory activity of r3 mesenchyme (Fig. 3), compared with PBS-treated or CH-ase buffer-only-treated (not shown) control cryosections. The CH-ase data suggest that the inhibitory activity could be due to either a CSPG or a CSPG-binding molecule. However, the latter suggestion is favoured by the observation that the activity can be eluted from cryosections by washing with CS-C or hypertonic saline.

By contrast, pretreatment of E10 wild-type cryosections with Pi-PLC, heparin, heparitinase, or CS-A (composed chiefly of chondroitin 4-sulphate chains) had no significant effect on the proportion of neurites which grew onto r3 mesenchyme (Fig. 3), suggesting that the activity is not GPI-linked to cell membranes, is unlikely to be a HSPG or HSPG-binding molecule, and may preferentially bind to C6SPG, rather than chondroitin-4-sulphated ones. In comparison to untreated cryosections, we found that all of the pretreatments appeared to reduce the potency of the r3 mesenchyme barrier to some extent, suggesting that although the activity may associate with certain sulphated proteoglycans, it is not firmly anchored to the mesenchyme (Fig. 3). Importantly, none of the pretreatments had any significant effect on the proportion of neurites which grew out from r3 mesenchyme onto the adjacent r2/r4 mesenchyme, indicating that the pretreatments were not unspecifically modifying the hindbrain substrate.

Following CS-A, CS-C, or PBS pretreatment, some cryosections were immunostained with a chondroitin sulphate-specific antibody (CS-56). All three treatments yielded identical patterns of immunostaining (not shown, but resembling the immunostaining shown in Fig. 5C), indicating that applied soluble CS did not bind to cryosections and thereby create an artificially uniform CS "carpet." We confirmed that heparitinase was digesting HSPGs within the cryosections and releasing UV-absorbing uronic acid residues by measuring the UV-absorbance of the enzyme solution at 232 nm before and after digestion. The efficacy of CH-ase digestion was confirmed by immunostaining CH-ase-treated cryosections with CS-56 antibody. CH-ase treatment markedly reduced CSPG immunoreactivity within the cryosections by 65–75% (quantified from CCD camera-digitised epifluorescence images).

In addition to digesting CSPG, CH-ase is also known to digest the glycosaminoglycan hyaluron (Yamagata *et al.*, 1968). Therefore, to exclude the possibility that the observed effects of CH-ase treatment were due to hyaluron degradation, some cryosections were pretreated with the hyaluron-specific degrading enzyme hyaluronidase. This pretreatment caused no significant increase in the proportion of neurites which grew onto r3 mesenchyme (33.0 $\pm$ 5.2%, 27 neurites, $n = 3$).

Neurites Readily Enter r3 Mesenchyme in erbB4 −/− Embryos

A previous study (Gassmann *et al.*, 1995) has shown that in mice which lack functional erbB4 receptor, centrally projecting trigeminal and facial/acoustic ganglia axons grow inappropriately into r3 mesenchyme. In this study, to determine whether r3 mesenchyme of erbB4 −/− mice lacks an axon growth-inhibitory activity, we cultured E10 wild-type trigeminal neurons on cryosections of E10 erbB4 −/− head. In contrast to the failure of neurites to grow onto wild-type r3 mesenchyme, we found that on erbB4 −/− cryosections neurons readily extended neurites from r2/r4 mesenchyme onto r3 mesenchyme (Fig. 4). Unlike wild-type cryosections, the proportion of neurites which grew

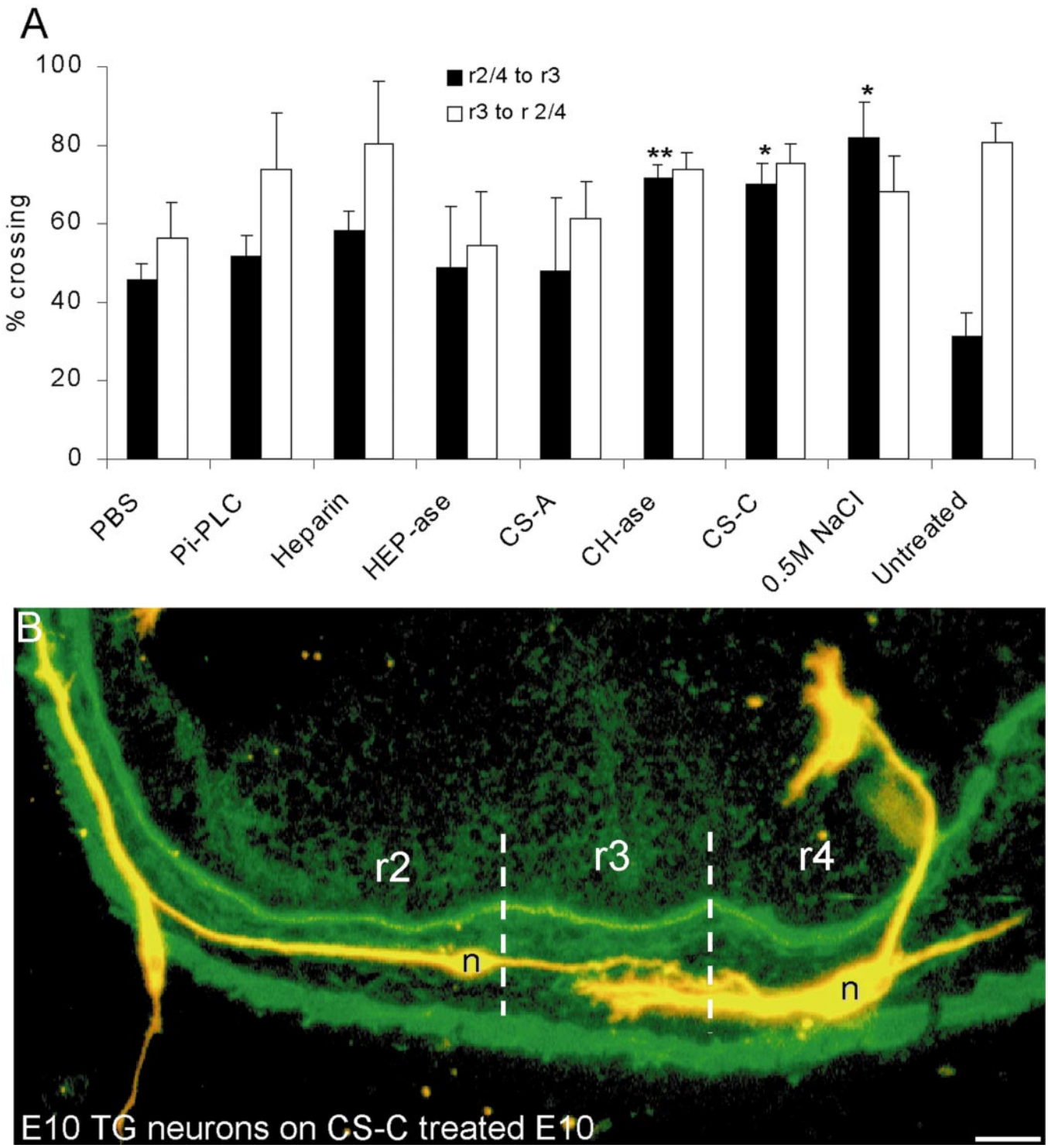

FIG. 3. Certain pretreatments of wild-type E10 cryosections remove the r3 mesenchyme neurite growth inhibitor. (A) Pretreating cryosections with chondroitinase (CH-ase), chondroitin sulphate-C (CS-C), or 0.5 M NaCl increased the proportion of neurites which extended onto r3 mesenchyme from r2 mesenchyme or r4 mesenchyme, compared with PBS-treated controls (black bars). However, pretreatment with phospholipase-C (Pi-PLC), heparin, heparitinase (HEP-ase), or chondroitin sulphate-A (CS-A) had no significant effect on the proportion of neurites which extended onto r3 mesenchyme. The r3 mesenchyme barrier was at its most potent on untreated cryosections which had not been pretreated with any solution. The proportion of neurites which grew from r3 mesenchyme onto the

onto erbB4 −/− r3 mesenchyme did not appear to be increased by pretreating these cryosections with CS-C (Fig. 4B).

Comparison of Proteoglycan Immunoreactivity in Wild-Type and erbB4 −/− Embryos

Because the wild-type r3 mesenchyme inhibitory activity appeared to associate with CSPG, we investigated the developmental expression of CSPG and C6SPG in E9–E10 wild-type and erbB4 −/− embryo hindbrains. In E9 wild-type embryos, CSPG immunoreactivity was present at rhombomere boundaries and was prominent within the neuroepithelial basal lamina and otic vesicle basal lamina and throughout the mesenchyme (Fig. 5A). By E10, CSPG immunoreactivity was reduced at rhombomere boundaries and within r2 mesenchyme and r4 mesenchyme at the sites of condensing sensory ganglia (as has been reported in the developing rat hindbrain by Morriss-Kay and Tuckett, 1989), although immunoreactivity remained prominent in the intervening mesenchyme adjacent to r3 (Figs. 5C and 5D). In E9 erbB4 −/− embryos, CSPG immunoreactivity appeared identical to that in wild-type embryos (Fig. 5B). Anti-C6SPG immunostained the same regions as anti-CSPG and no differences were detected between the staining patterns in wild-type or erbB4 −/− embryos (data not shown). In head cryosections of wild-type E10 embryos, HSPG immunoreactivity was present at rhombomere boundaries and within the neuroepithelial basal lamina, otic vesicle basal lamina, and blood vessels (Fig. 5E). We detected no differences in the intensity or distribution of HSPG immunoreactivity between head cryosections of either wild-type (Fig. 5E) or erbB4 −/− (Fig. 5F) embryos. HSPG immunoreactivity closely resembled laminin immunoreactivity (compare with Figs. 1–4) and, unlike CSPG immunoreactivity, we detected relatively little HSPG immunoreactivity within the cranial mesenchyme in either wild-type or erbB4 −/− embryos (compare Figs. 5E and 5F with Fig. 5C).

Spatiotemporal Expression of erbB4 mRNA in Wild-Type Hindbrain

To further investigate the link between erbB4 expression and the onset of the r3 mesenchyme barrier, we performed erbB4 *in situ* hybridisation on E9 and E10 wild-type embryos. At E9, erbB4 mRNA was present throughout the rostrocaudal extent of r3 and r5 neuroepithelium, although it was most prominent dorsally and at the rhombomere boundaries (Fig. 6A). In transverse sections through r3 and r5, near their boundaries with r4, erbB4 expression was observed within the proliferative ventricular zone (Figs. 6B and 6C) and throughout the thickness of the dorsal third of the neuroepithelium in r5 (Fig. 6C), whilst in the dorsal third of r3 it was displaced marginally to the rhombic lip and the pial surface (Fig. 6B). Further rostrally, erbB4 mRNA was detected in a continuum from r1 to the forebrain (Fig. 6A).

By E10, erbB4 mRNA became further focussed to the rhombomere boundaries in r3 and r5, whilst the expression from r1 into the forebrain remained continuous (Fig. 6D). In transverse sections through r1, r3, and r5 (Figs. 6E–6G, respectively) erbB4 expression was now undetectable in the ventricular zone and was instead concentrated at the pial surface and possibly within the pia itself, predominantly just ventral to the adjacent nerve entry points in r2 and r4. Strong erbB4 expression was also observed in the roof plate of r1, r3, and r5 (Fig. 6E–6G). Thus, erbB4 expression in r3 (and r5) shifts towards (but not into) the mesenchyme and concentrates at the rhombomere boundaries during the same period as the r3 mesenchyme axon barrier increases in potency.

ErbB4 Does Not Directly Inhibit Neurite Growth

In our cryoculture experiments, neurites growing within the mesenchyme were sometimes observed to grow along the pial basal lamina. Although we were able to show that in E10 wild-type embryos erbB4 was not expressed within r3 mesenchyme (Fig. 6), we could not exclude the possibility that erbB4 was expressed by some r3 pial cells (Figs. 6E–6G). Thus, it remained possible that erbB4 might be directly responsible for inhibiting the growth of some neurites into r3 mesenchyme territory. To test this hypothesis, two control experiments were performed. In the first, cryocultures of E10 wild-type head cryosections were maintained in the presence of an antibody which masks the extracellular domain of erbB4 (Chen *et al.*, 1996). The proportion of neurites which grew from r2/r4 mesenchyme onto r3 mesenchyme under these conditions (35.9 ± 5.6%, 38 neurites, $n = 3$) did not differ significantly from untreated cryocultures or from control cryocultures in which normal mouse serum was used instead of anti-erbB4 (34.3 ± 6.7%, 23 neurites, $n = 4$). In the second experiment, an erbB4-Fc fusion protein was laid down in a pattern on glass coverslips which were then used as a growth substrate for

adjacent r2/r4 mesenchyme (clear bars) was not significantly altered by any of the pretreatments. (B) E10 cryosection pretreated with CS-C and then seeded with E10 trigeminal ganglion neurons (n), cultured overnight, and immunostained with anti-laminin antibody (green) and anti-β3-tubulin antibody (orange). In contrast to untreated cryosections (compare with Fig. 1D), neurites readily grow onto CS-C-treated r3 mesenchyme (bounded by dashed lines). Error bars in A are ± SEM; $^*P < 0.05$ and $^{**}P < 0.01$ significant difference from PBS control value, with Bonferroni correction. All experimental conditions were repeated in triplicate, except for PBS (four times), CS-A (four times), CS-C (eight times), heparin (four times), and untreated (nine times). Bar in B, 50 μm.

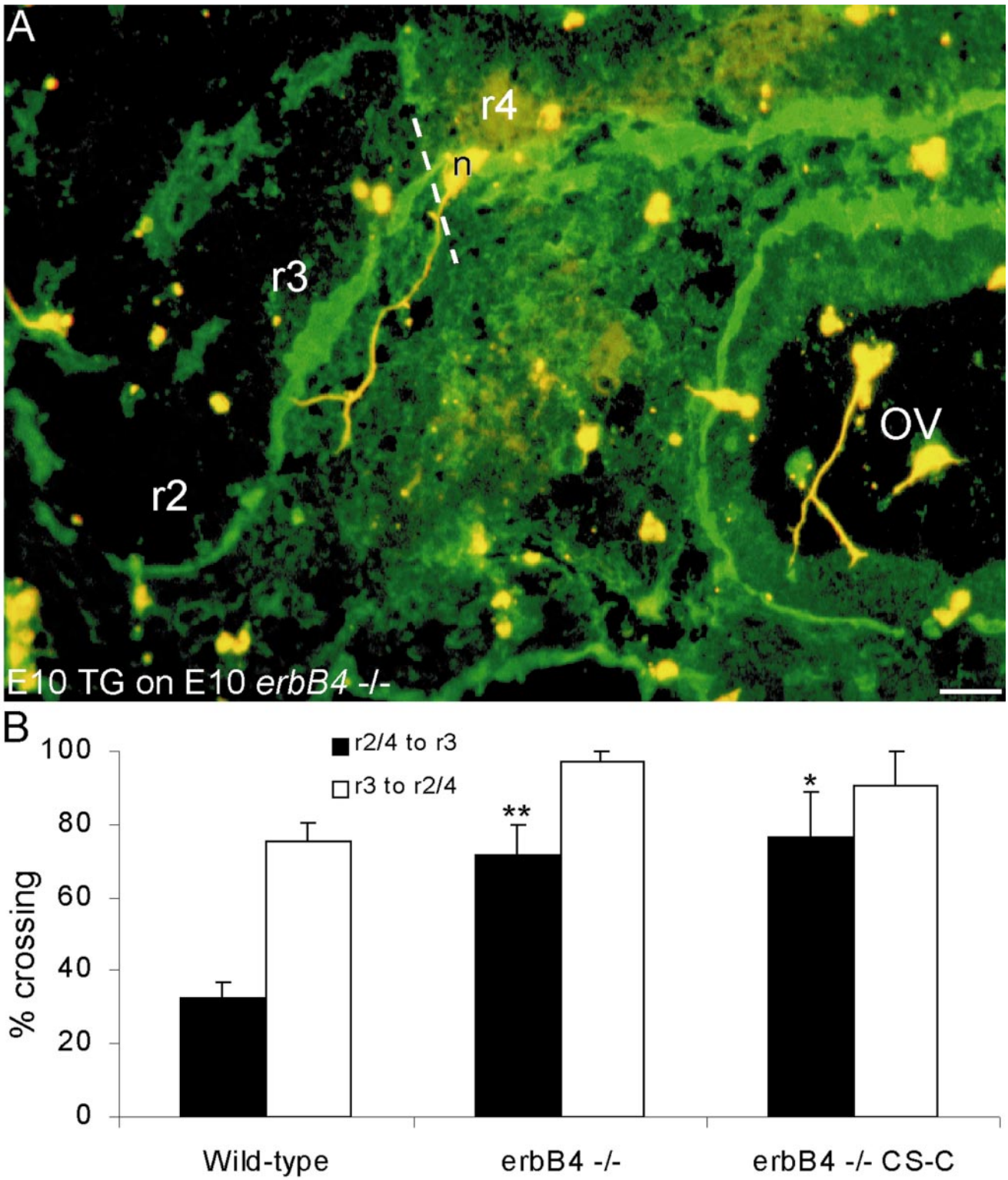

FIG. 4. Mesenchyme adjacent to r3 is not a barrier to sensory neurite growth in erbB4 −/− embryos. (A) Wild-type E10 trigeminal ganglion neurons (n) (stained orange with anti-β3-tubulin antibody) growing neurites on an E10 erbB4 −/− head cryosection (stained green with anti-laminin antibody). A neurite can be seen to grow from r4 mesenchyme onto r3 mesenchyme (boundary between r3 and r4 marked with

dissociated trigeminal neurons. The proportion of neurites which grew into the erbB4-containing regions (50.2 ± 2.6%, 247 neurites, $n = 3$) was no different from the proportion of neurites which grew into similar regions, containing human IgG as a control (53.4 ± 6.7%, 62 neurites, $n = 3$). Both of these data indicate that erbB4 does not directly inhibit trigeminal neurite growth.

DISCUSSION

It is now widely accepted that axons navigate to their appropriate targets in development by responding to growth-attractive/promoting and growth-repulsive/inhibitory molecules. However, in most instances the relative contributions of these cues remain unknown. In this study we demonstrate that centrally projecting trigeminal sensory axons (and trigeminal motor axons) might be constrained to their appropriate pathway within r2 mesenchyme by a CSPG-binding axon growth-inhibitory activity within the neighbouring r3 mesenchyme. Moreover, the production of this inhibitory activity may require signalling events transduced via the neuregulin receptor erbB4, concentrated towards the pial surface and rhombomere boundaries within r3.

The presence of an axon growth-inhibitory activity in r3 mesenchyme is consistent with an earlier study which proposed that r3 mesenchyme and r5 mesenchyme constitute axon growth "exclusion zones" (Keynes *et al.*, 1991). In those experiments, when the neuroepithelium was displaced caudally, such that axon entry/exit points in r2 and r4 abutted r3 mesenchyme and r5 mesenchyme, respectively, motor axons seldom grew out into the mesenchyme. In agreement with this observation, we similarly found that neurons isolated from r2 and r3 neuroepithelium seldom grew into r3 mesenchyme, although neurites of telencephalic neurons exhibited no such preferential growth. Therefore, although the cranial mesenchyme is not segmented anatomically, it may be segmented molecularly into growth-permissive and growth-inhibitory regions, to which only specific classes of sensory and motor axons are responsive, and this segmentation may be specified by signals derived from the adjacent segmented neuroepithelium.

Cranial sensory ganglia begin to form from E8.5 in the mouse and centrally projecting sensory axons grow from these ganglia towards the hindbrain neuroepithelium from E9.5 (Davies and Lumsden, 1984; Stainier and Gilbert, 1990). The timing of this initial axon growth correlates with the appearance of the axon growth-inhibitory activity in r3 mesenchyme around E9, suggesting that it may have a role in constraining the growth of the earliest centrally projecting trigeminal axons. Between E9 and E10, when the majority of centrally projecting axons are growing, the inhibitory activity increases in potency and this coincides with a shift in the distribution of erbB4-expressing cells towards the pial surface of the r3 neuroepithelium and thus closer to the overlying r3 mesenchyme. The axon-pathfinding defects seen in erbB4 −/− embryos are unlikely to be related to any loss of this erbB4-expressing cell population, since the truncated erbB4 mRNA transcripts produced by erbB4 −/− embryos (which encode a biologically inactive form of erbB4) can be detected by *in situ* hybridisation and show an identical distribution to the full-length erbB4 transcripts in wild-type embryos (data not shown). Furthermore, our experiments with an erbB4-Fc fusion protein and a function-blocking antibody to the extracellular domain of erbB4, together with the observation that erbB4 mRNA is not expressed within r3 mesenchyme, suggest that erbB4 itself is not the axon growth-inhibitory activity. Indeed, a previous study found that the erbB4–Fc fusion protein actually potentiated neurite outgrowth (Pinkas-Kramarski *et al.*, 1997).

Although erbB4 does not directly inhibit axon growth, it remains possible that signalling events mediated by erbB4 generate the r3 mesenchyme-inhibitory activity. Consistent with this scheme, between E8 and E10 r2, r4, and r6 neuroepithelium express an erbB4 ligand, the transmembrane type I isoform of neuregulin (Meyer *et al.*, 1997). Thus, sites of neuregulin expression directly abut sites of receptor expression in neighbouring rhombomeres. Neuregulin is also expressed throughout the hindbrain in a thin layer of cells lying at, or just outside, the pial surface of the neuroepithelium (Meyer and Birchmeier, 1994). These marginal cells lie close to, and may even be identical to, the erbB4-expressing cells we find at the pial surface of the neuroepithelium. We therefore propose that erbB4-mediated signalling in cells at the margins of r3 induces these cells either to secrete an axon growth-inhibitory activity or to secrete a signalling molecule which induces the neighbouring r3 mesenchyme to produce an axon growth-inhibitory activity. Furthermore, our ability to displace an inhibitory activity from wild-type cryosections with CH-ase and CS-C, but not CS-A, suggests that it is not a CSPG, but more likely binds to CSPGs and especially C6SPGs. However, our initial attempts to extract this

dashed line). (B) Quantification of the growth of wild-type neurites from r2 mesenchyme or r4 mesenchyme onto r3 mesenchyme in either wild-type or erbB4 −/− cryosections (black bars) indicates that a significantly higher proportion of neurites enter erbB4 −/− r3 mesenchyme. Unlike wild-type cryosections, pretreatment of erbB4 −/− head cryosections with chondroitin sulphate-C (CS-C) fails to further increase the proportion of neurites which grow into r3 mesenchyme. Error bars are ± SEM; $*P < 0.05$ and $**P < 0.01$ significant difference from wild-type value, with Bonferroni correction. Wild-type data are the mean of nine independent experiments, whilst erbB4 −/− and erbB4 −/− CS-C experiments were repeated five and three times, respectively. OV, otic vesicle. Bar in A, 50 μm.

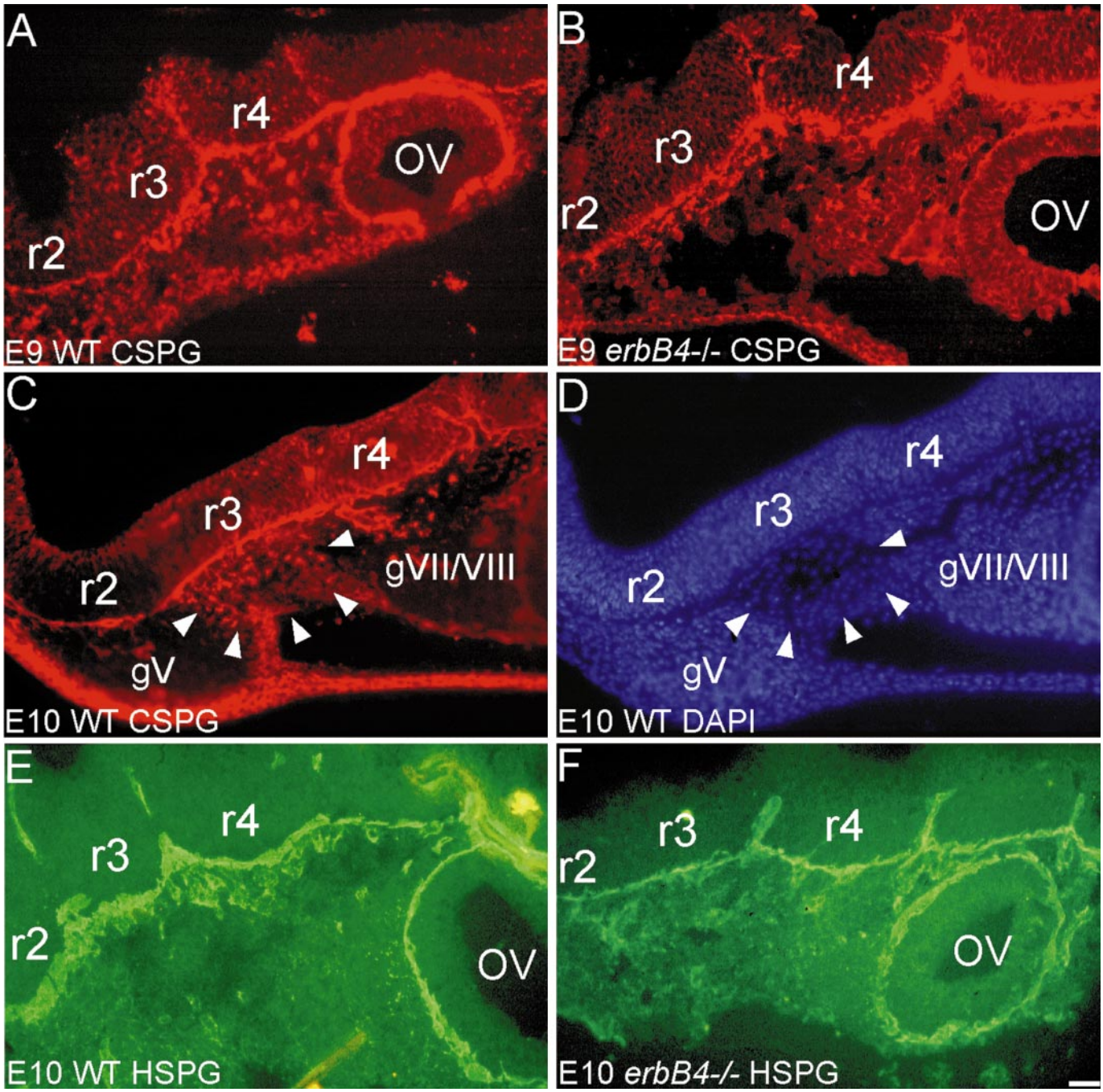

FIG. 5. Distribution of chondroitin-sulphated proteoglycans (CSPG) and heparan-sulphated proteoglycans (HSPG) in E9–E10 wild-type and erbB4 −/− embryos. (A–D) At all ages examined CSPG immunoreactivity (A–C) delineates the basal lamina of the neurepithelium, boundaries between rhombomeres, and areas of the cranial mesenchyme. Between E9 (A) and E10 (C) CSPG immunoreactivity becomes reduced within the forming cranial ganglia (gV and gVII/VIII) and concentrated in the area adjacent to r3 (within the area bounded by arrowheads in C and the corresponding area shown counterstained with DAPI nuclear stain in D). CSPG immunoreactivity in the E9 erbB4 −/− hindbrain (B) does not differ from that in wild-type embryos (compare A and B). (E, F) At E10, HSPG immunoreactivity was similar to that of CSPG, but was comparatively sparse in the cranial mesenchyme. No differences in HSPG immunoreactivity were detected between wild-type (E) and erbB4 −/− (F) embryos. OV, otic vesicle; gV, trigeminal ganglion; gVII/VIII, facial/acoustic ganglia. Bars, 50 μm.

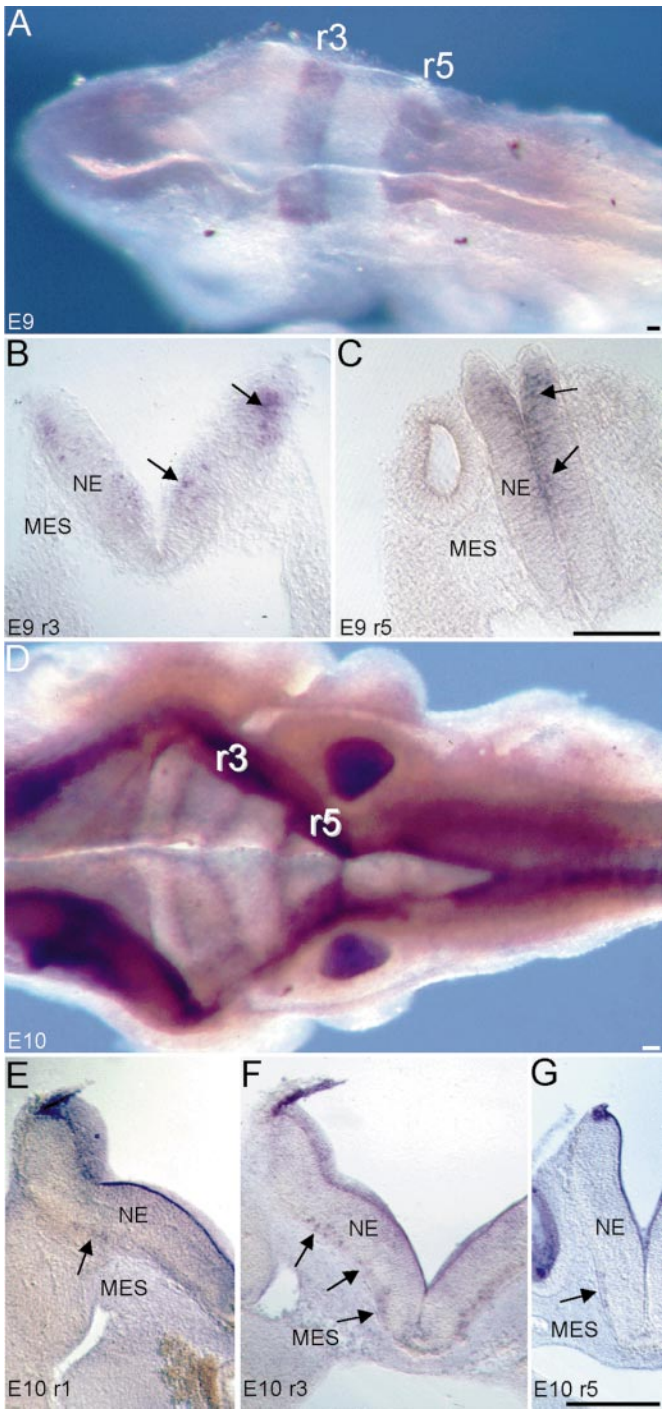

FIG. 6. ErbB4 mRNA becomes expressed in cells abutting the mesenchyme. At E9 (A–C) erbB4 is expressed in neuroepithelial cells extending from r1 into the forebrain and also within r3 and r5, where it is slightly more concentrated towards the rhombomere boundaries. Transverse sections through r3 (B) and r5 (C) demonstrate that erbB4 is expressed in the ventricular zone and throughout the thickness of the dorsal neuroepithelium (arrows). By E10 (D–G) erbB4 mRNA has become highly concentrated at the rhombomere boundaries in r3 and r5. In transverse sections through r1 (E), r3 (F), and r5 (G), it can be seen that the expression of erbB4 has shifted to the pial surface of the neuroepithelium (arrows). Strong expression is also seen in the roof plate. NE, neuroepithelium; MES, mesenchyme. Bars, 50 μm.

growth-inhibitory activity from wild-type hindbrains and bind it to patterned substrates of CS-C or CS-A in *in vitro* stripe assays have not produced any conclusive effect. No doubt very many CSPG-binding molecules are present in the tissue extracts, only a small number of which may be inhibitory for axon growth. Therefore, although suggestive, our data do not yet provide a direct link between the erbB4 phenotype and the chemical pretreatment phenotype, and it is possible that these could be mechanistically unrelated. The ability of CSPG-binding molecules to affect the pattern of neurite growth has previously been demonstrated in the developing mouse cerebral cortex (Emerling and Lander, 1996) and retina (Brittis and Silver, 1994). Throughout the hindbrain we found that C6SPG immunoreactivity colocalised with CSPG in mesenchyme and basement membranes at all ages studied (E8–E10), and no differences were detected in the distribution of C6SPG or CSPG between wild-type and erbB4 $-/-$ embryos. This also suggests that sulphated proteoglycans might not be directly responsible for the inhibition of axon growth by r3 mesenchyme. However, some studies have shown that different CSPGs can either inhibit (Fernaud-Espinosa *et al.*, 1998) or promote (Faissner *et al.*, 1994) neurite growth, and it remains possible that distinct forms of CSPGs may be regionally distributed within the cranial mesenchyme. In contrast to CSPGs, HSPGs are generally associated with axon growth-permissive areas of vertebrate embryos (Walz *et al.*, 1997; Treloar *et al.*, 1996). In agreement with this scheme, we detected relatively little HSPG within cranial mesenchyme and enzymatic digestion of HSPG in cryosections or washing with heparin did not markedly disrupt the inhibitory activity. The lack of a significant effect in our experiments with heparin washes is perplexing, given that heparin generally destabilises most protein–GAG interactions. However, our data show that heparin washes do have a partial effect, increasing the proportion of neurites that grow into r3 mesenchyme by 12.5% above control levels (Fig. 3), although this increase was not significant (P = 0.09). Furthermore, there is evidence that at least some protein–CSPG interactions can be disrupted by soluble CS, but are barely affected by soluble heparin (Blase *et al.*, 1996). It therefore seems that the inhibitory activity we describe is predominantly bound to C6S.

Other potential candidates for the r3 mesenchyme growth-inhibitory activity include the ephrin and Eph receptor family of guidance molecules, which have been implicated in patterning neural crest cell migration (Krull *et al.*, 1997) and motor axon outgrowth in the developing spinal cord (Flanagan and Vanderhaeghen, 1998; Wang and

Anderson, 1997). The failure of Pi-PLC to remove the r3 mesenchyme activity in our experiments suggests that the GPI-linked forms of ephrins (A-type) are probably not involved, although further studies on the possible involvement of transmembrane ephrins (B-type) are in progress.

In conclusion, we show that the embryonic cranial mesenchyme is far from simply being a homogeneous "support matrix" for growing axons, but instead is segmented molecularly into axon growth-permissive and growth-inhibitory zones, possibly under the influence of erbB4-mediated signals. Future work will now be directed at revealing the identity and mechanism of action of this growth inhibitor.

ACKNOWLEDGMENTS

We thank Yosef Yarden for ErbB4-Fc reagent and Greg Lemke and David Wilkinson for critically reviewing the manuscript. This work is funded by the Medical Research Council.

REFERENCES

Blase, L., Merling, A., Engelmann, S., Moller, P., and Schwartz-Albiez, R. (1996). Characterization of cell surface-expressed proteochondroitin sulfate of pre-B Nalm-6 cells and its possible role in laminin adhesion. *Leukemia* **10,** 1000–1011.

Brittis, P. A., and Silver, J. (1994). Exogenous glycosaminoglycans induce complete inversion of retinal ganglion-cell bodies and their axons within the retinal neuroepithelium. *Proc. Natl. Acad. Sci. USA* **91,** 7539–7542.

Chen, X., Levkowitz, G., Tzahar, E., Karunagaran, D., Lavi, S., Ben-Baruch, N., Leitner, O., Ratzkin, B. J., Bacus, S. S., and Yarden, Y. (1996). An immunological approach reveals biological differences between the two NDF/heregulin receptors, ErbB3 and ErbB4. *J. Biol. Chem.* **271,** 7620–7629.

Chiba, A., and Keshishian, H. (1996). Neuronal pathfinding and recognition: Roles of cell adhesion molecules. *Dev. Biol.* **180,** 424–432.

Culotti, J. G., and Kolodkin, A. L. (1996). Functions of netrins and semaphorins in axon guidance. *Curr. Opin. Neurobiol.* **6,** 81–88.

Davies, A., and Lumsden, A. G. S. (1984). Relation of target encounter and neuronal death to nerve growth factor responsiveness in the developing mouse trigeminal ganglion. *J. Comp. Neurol.* **223,** 124–137.

Davies, A. M. (1996). Cranial sensory neurons. *In* "Neural Cell Culture" (J. Cohen and G. P. Wilkin, Eds.), pp. 153–175. IRL Press, Oxford.

Emerling, D. E., and Lander, A. D. (1996). Inhibitors and promoters of thalamic neuron adhesion and outgrowth in embryonic neocortex: Functional association with chondroitin sulfate. *Neuron* **17,** 1089–1100.

Faissner, A., Clement, A., Lochter, A., Streit, A., Mandl, C., and Schachner, M. (1994). Isolation of a neural chondroitin sulfate proteoglycan with neurite outgrowth-promoting properties. *J. Cell Biol.* **126,** 783–799.

Fernaud-Espinosa, I., Nieto-Sampedro, M., and Bovolenta, P. (1998). A neurite outgrowth-inhibitory proteoglycan expressed during development is similar to that isolated from adult brain after isomorphic injury. *J. Neurobiol.* **36,** 16–29.

Flanagan, J. G., and Vanderhaeghen, P. (1998). The ephrins and Eph receptors in neural development. *Annu. Rev. Neurosci.* **21,** 309–345.

Gassmann, M., Casagranda, F., Orioli, D., Simon, H., Lai, C., Klein, R., and Lemke, G. (1995). Aberrant neural and cardiac development in mice lacking the erbB4 neuregulin receptor. *Nature* **378,** 390–394.

Gavalas, A., Davenne, M., Lumsden, A., Chambon, P., and Rijli, F. M. (1997). Control of axon guidance and rostral hindbrain patterning by *Hoxa-2*. *Development* **124,** 3693–3702.

Grumet, M., Friedlander, D. R., and Sakurai, T. (1996). Functions of brain chondroitin sulfate proteoglycans during development: Interactions with adhesion molecules. *Perspect. Dev. Neurobiol.* **3,** 319–330.

Hantaz-Ambroise, D., Vigny, M., and Koenig, J. (1987). Heparan sulfate proteoglycan and laminin mediate two different types of neurite outgrowth. *J. Neurosci.* **7,** 2293–2304.

Keynes, R., and Cook, G. M. W. (1995). Axon guidance molecules. *Cell* **83,** 161–169.

Keynes, R., Tannahill, D., Morgenstern, D. A., Johnson, A. R., Cook, G. M. W., and Pini, A. (1997). Surround repulsion of spinal sensory axons in higher vertebrate embryos. *Neuron* **18,** 889–897.

Keynes, R. J., Jaques, K. F., and Cook, G. M. W. (1991). Axon repulsion during peripheral nerve segmentation. *Development* **Suppl. 2,** 131–140.

Krull, C. E., Lansford, R., Gale, N. W., Collazo, A., Marcelle, C., Yancopoulos, G. D., Fraser, S. E., and Bronner-Fraser, M. (1997). Interactions of Eph-related receptors and ligands confer rostrocaudal pattern to trunk neural crest migration. *Curr. Biol.* **7,** 571–580.

Lumsden, A., and Krumlauf, R. (1996). Patterning the vertebrate neuraxis. *Science* **274,** 1109–1115.

Margolis, R. U., and Margolis, R. K. (1997). Chondroitin sulfate proteoglycans as mediators of axon growth and pathfinding. *Cell Tissue Res.* **290,** 343–348.

Meyer, D., and Birchmeier, C. (1994). Distinct isoforms of neuregulin are expressed in mesenchymal and neuronal cells during mouse development. *Proc. Natl. Acad. Sci. USA* **91,** 1064–1068.

Meyer, D., Yamaai, T., Garratt, A., Riethmacher-Sonnenberg, E., Kane, D., Theill, L. E., and Birchmeier, C. (1997). Isoform-specific expression and function of neuregulin. *Development* **124,** 3575–3586.

Morriss-Kay, G., and Tuckett, F. (1989). Immunohistochemical localisation of chondroitin sulphate proteoglycans and the effects of chondroitinase ABC in 9- to 11-day rat embryos. *Development* **106,** 787–798.

Niederlander, C., and Lumsden, A. (1996). Late emigrating neural crest cells migrate specifically to the exit points of cranial branchiomotor nerves. *Development* **122,** 2367–2374.

Nieto, M. A. (1996). Molecular biology of axon guidance. *Neuron* **17,** 1039–1048.

Oakley, R. A., and Tosney, K. W. (1991). Peanut agglutinin and chondroitin-6-sulfate are molecular markers for tissues that act as barriers to axon advance in the avian embryo. *Dev. Biol.* **147,** 187–206.

Pinkas-Kramarski, R., Eilam, R., Alroy, I., Levkowitz, G., Lonai, P., and Yarden, Y. (1997). Differential expression of NDF/neuregulin receptors ErbB-3 and ErbB-4 and involvement in inhibition of neuronal differentiation. *Oncogene* **15,** 2803–2815.

Schneider-Maunoury, S., Seitanidou, T., Charnay, P., and Lumsden, A. (1997). Segmental and neuronal architecture of the hindbrain of Krox-20 mouse mutants. *Development* **124,** 1215–1226.

Silver, J. (1994). Inhibitory molecules in development and regeneration. *J. Neurol.* **242**(Suppl). S22–S24.

Snow, D. M., Watanabe, M., Letourneau, P. C., and Silver, J. (1991). A chondroitin sulfate proteoglycan may influence the direction of retinal ganglion cell outgrowth. *Development* **113,** 1473–1485.

Stainier, D. Y. R., and Gilbert, W. (1990). Pioneer neurons in the mouse trigeminal sensory system. *Proc. Natl. Acad. Sci. USA* **87,** 923–927.

Studer, M., Lumsden, A., Ariza-McNaughton, L., Bradley, A., and Krumlauf, R. (1996). Altered segmental identity and abnormal migration of motor neurons in mice lacking Hoxb-1. *Nature* **384,** 630–634.

Tonge, D. A., Golding, J. P., Edbladh, M., Kroon, M., Ekstrom, P. E. R., and Edstrom, A. (1997). Effects of extracellular matrix components on axonal outgrowth from peripheral nerves of adult animals in vitro. *Exp. Neurol.* **146,** 81–90.

Treloar, H. B., Nurcombe, V., and Key, B. (1996). Expression of extracellular matrix molecules in the embryonic rat olfactory pathway. *J. Neurobiol.* **31,** 41–55.

Tucker, A., Lumsden, A., and Guthrie, S. (1996). Cranial motor axons respond differently to the floor plate and sensory ganglia in collagen gel co-cultures. *Eur. J. Neurosci.* **8,** 906–916.

Walsh, F. S., and Doherty, P. (1997). Neural cell adhesion molecules of the immunoglobulin superfamily: Role in axon growth and guidance. *Annu. Rev. Cell Dev. Biol.* **13,** 425–456.

Walz, A., McFarlane, S., Brickman, Y. G., Nurcombe, V., Bartlett, P. F., and Holt, C. E. (1997). Essential role of heparan sulfates in axon navigation and targeting in the developing visual system. *Development* **124,** 2421–2430.

Wang, H. U., and Anderson, D. J. (1997). Eph family transmembrane ligands can mediate repulsive guidance of trunk neural crest migration and motor axon outgrowth. *Neuron* **18,** 383–396.

Wilkinson, D. G., and Nieto, M. A. (1993). Detection of messenger-RNA by in-situ hybridization to tisue sections and whole mounts. *Methods Enzymol.* **225,** 361–373.

Yamagata, T., Saito, H., Habuchi, O., and Suzuki, S. (1968). Purification and properties of bacterial chondroitinases and chondrosulfatases. *J. Biol. Chem.* **243,** 1523–1535.

Received for publication April 2, 1999
Revised September 10, 1999
Accepted September 13, 1999